

# Superfluidity versus Disorder in the Discrete Nonlinear Schrödinger Equation

A. Trombettoni<sup>1,2</sup>, A. Smerzi<sup>1,2</sup> and A.R. Bishop<sup>1</sup>

<sup>1</sup> Theoretical Division and Center for Nonlinear Studies, Los Alamos National Laboratory, Los Alamos, NM 87545 USA

<sup>2</sup> Istituto Nazionale di Fisica per la Materia and International School for Advanced Studies,  
via Beirut 2/4, I-34014, Trieste, Italy

(November 10, 2018)

We study the discrete nonlinear Schrödinger equation (DNLS) in an annular geometry with on-site defects. The dynamics of a traveling plane-wave maps onto an effective "non-rigid pendulum" Hamiltonian. The different regimes include the complete reflection and refocusing of the initial wave, solitonic structures, and a superfluid state. In the superfluid regime, which occurs above a critical value of nonlinearity, a plane-wave travels coherently through the randomly distributed defects. This superfluidity criterion for the DNLS is analogous to (yet very different from) the Landau superfluidity criteria in translationally invariant systems. Experimental implications for the physics of Bose-Einstein condensate gases trapped in optical potentials and of arrays of optical fibers are discussed.

PACS: 42.82.Et, 05.45.-a, 03.75.Fi

Studying the interplay between nonlinearity and disorder has become a fundamental issue of the last decades in the study of many physical and biological systems (both discrete and continuous) [1]. It is well known that nonlinearity *or* disorder may lead to localized excitations - 'solitonic' structures [2] and 'Anderson localization' [3], respectively. However, the dynamical properties of the system, when both nonlinearity *and* disorder are present, are still challenging theoretical investigations. This problem is, moreover, of central experimental relevance, since impurities can be reduced but never completely eliminated. In particular, it can be asked if random defects will (and, if so, how) destroy the propagation of traveling plane waves or localized excitations (allowed by the nonlinearity), and what are the conditions for crossing from a "superfluid" regime with propagation (and coherence) preserved (due to, for instance, a large nonlinearity), to a "normal" regime with disorder induced damping.

Here, we consider the dynamical properties of the DNLS in an annular geometry and in the presence of impurities. We choose the DNLS for two main reasons: 1) it has all the required ingredients: nonlinearity, disorder and discreteness; 2) real physical systems, such as optical fibers and Bose-Einstein condensates in deep optical lattices, map onto the DNLS and provide an ideal experimental framework. The annular geometry is paradigmatic for studying the nature of superfluidity [4], and allows a clear comparison between the discrete and continuous (translationally invariant) limits.

With regard to optical fibers, a typical experimental setup is an array of one dimensional nonlinear coupled waveguides [5]. As the light propagates through the array, the coupling induces an exchange of power among the single waveguides. In the low power limit (i.e. when the nonlinearity is negligible), the optical field spreads over the whole array. Upon increasing the power, the output field narrows until it is localized in a few waveguides, and discrete solitons can finally be observed [5,6].

The evolution of  $E_n(\tau)$ , the electrical field in the  $n$ th waveguide, as a function of the position,  $\tau$ , is governed by the DNLS Eq.(1). In this case  $\Lambda$  is proportional to the Kerr nonlinearity and the on-site potentials  $\epsilon_n$  are the effective refraction indices of the individual waveguides. In [7] a linearly growing  $\epsilon_n$  was realized, which allowed the observation of Bloch oscillations.

Another significant physical system described by the DNLS is a Bose-Einstein condensate (BEC) gas confined in a deep optical lattice. A one dimensional optical lattice can be created experimentally by a far-detuned, retro-reflected laser beam [8–11]. The condensate wavefunction  $\psi(\vec{r}, t)$  obeys the Gross-Pitaevskii equation [12] which is a (continuous) nonlinear Schrödinger equation, with the nonlinearity arising from the interatomic interaction. When the heights of the intra-well barriers of the periodic optical potential are much higher than the condensate chemical potential, the system can be mapped onto the DNLS Eq.(1) [13], with  $\psi_n$  the condensate amplitude in the  $n$ th well and  $\epsilon_n$  proportional to any external field superimposed on the lattice. In [8] a coherent output of matter waves was created by a vertical optical array (with the gravity gradient providing  $\epsilon_n \propto n$ ). In [10], the magnetic trap and the laser beams were turned on in a superimposed harmonic magnetic field ( $\epsilon_n \propto n^2$ ), allowing the direct observation of coherent (Josephson) condensate oscillations governed by Eq. (1).

The DNLS is (in dimensionless units):

$$i \frac{\partial \psi_n}{\partial \tau} = -\frac{1}{2}(\psi_{n-1} + \psi_{n+1}) + (\epsilon_n + \Lambda |\psi_n|^2) \psi_n, \quad (1)$$

where  $\Lambda$  is the nonlinear coefficient and  $n = 1, \dots, N$  ( $N$  number of sites). In the physical systems we have discussed, the defects  $\epsilon_n$  can be spatially localized or extended. For instance, the impurities in optical fibers can be induced by different (possibly random) effective refraction indexes of the guides or with varying spatial separations between them. In BEC's the defects can be

created with additional lasers and/or magnetic fields; the presence of a thermal component can also be phenomenologically modeled, in some limits, by a random distribution of defects.

We consider, first, the DNLS with a single impurity  $\epsilon_n = \epsilon \delta_{n,\bar{n}}$  at the site  $\bar{n}$ , and study the propagation of a plane wave  $\psi_n(\tau = 0) = e^{ikn}$ . In the following we assume  $\Lambda > 0$  (which corresponds to a repulsive interatomic interaction in BEC's, as is the case for  $^{87}\text{Rb}$  atoms). Note, however, that Eq.(1) is invariant with respect to the transformation  $\Lambda \rightarrow -\Lambda$ ,  $\epsilon_n \rightarrow -\epsilon_n$ , and  $\psi_n \rightarrow \psi_n^* e^{i\pi n}$ . Since we consider periodic boundary conditions (due to the annular geometry), we have  $k = 2\pi l/N$  with  $l$  integer ( $l = 0, 1, \dots, N-1$ ).

In the translationally invariant limit of the DNLS, given by the continuum nonlinear Schrödinger equation (CNLS), a well known argument suggested by Landau implies that superfluidity occurs when the speed is smaller than the sound velocity (for weak perturbations). A simple derivation of the Landau critical velocity in the CNLS was recently proposed in [4] considering an annular geometry with a single (small) impurity. The key point was to map the problem of the propagation of a plane wave to a Josephson-like Hamiltonian. The superfluid regime is allowed by the nonlinearity, which provided an effective energy barrier against the creation of elementary excitations with momentum  $k+q, k-q$  (with  $q$  arbitrarily small) which would dissipate the energy of the incident wave having momentum  $k$ .

This scenario is completely changed by discreteness. First, it is well known that when  $\cos k < 0$  the system becomes modulationally unstable [14]. Stability analysis reveals that the eigenfrequencies of the linear modes become imaginary driving an exponential growth of small perturbations. This modulation instability disappear, for  $\Lambda > 0$ , in the CNLS limit. Let us consider, then, the case in which  $\cos k > 0$ . In the absence of the impurity, superpositions of rotational states with opposite wave-vectors  $k, -k$  are degenerate. The defect splits the degeneracy by coupling the two  $k, -k$  waves, very much as the tunneling barrier does in a double well potential, with "left" and "right" localized states. Therefore, the relative population of the two waves oscillates according to an effective (generalized [18]) Josephson Hamiltonian. These Josephson regimes are preserved as far as the splitting in energy induced by the defect  $\sim \epsilon$  is much smaller than the energy gap between different rotational states  $\sim 2\pi \sin k$ . In this limit, we can write the wavefunction  $\psi_n(\tau)$  as

$$\psi_n(\tau) = A(\tau) e^{ikn} + B(\tau) e^{-ikn}. \quad (2)$$

In the following, we set  $A, B = \sqrt{n_{A,B}(\tau)} e^{i\phi_{A,B}(\tau)}$ ,  $z = n_A - n_B$  and  $\phi = \phi_A - \phi_B$ . We will compare the numerical solution of (1) with the analytical solution of (3) obtained from the ansatz (2).

The two-mode Eq.(2) can be extended to the case of a time-dependent, arbitrary (including random) distribution of defects, with  $\epsilon$  replaced, as shown below, by an

effective impurity strength. Furthermore, when the initial wave function is given by the sum of multiple waves  $\psi_n(0) = \sum_j A_j e^{ik_j n}$ , the ansatz (2) can be straightforwardly generalized so long as the quasi-momentum distributions peaked around  $k_j$  do not overlap. The collision of a soliton with a single impurity has been studied, from a different perspective, in [15]. A numerical analysis of the propagation of plane waves across a segment with defects was made in [16].

Let us now derive the equations of motion. We define an effective Lagrangian as  $\mathcal{L} = \sum_n i\dot{\psi}_n \psi_n^* - \mathcal{H}$ , where  $\mathcal{H} = \sum_n [-\frac{1}{2}(\psi_n \psi_{n+1}^* + \psi_n^* \psi_{n+1}) + \epsilon_n |\psi_n|^2 + \frac{\Lambda}{2} |\psi_n|^4]$  (both the Hamiltonian  $\mathcal{H}$  and the norm  $\sum_n |\psi_n|^2 = N$  are conserved). The Euler-Lagrange equations  $\frac{d}{dt} \frac{\partial \mathcal{L}}{\partial \dot{q}_i} = \frac{\partial \mathcal{L}}{\partial q_i}$  for the variational parameters  $q_i(\tau) = n_{A,B}, \phi_{A,B}$  give the following equations:

$$\dot{z} = -\frac{2\epsilon}{N} \sqrt{1-z^2} \sin \phi \quad (3a)$$

$$\dot{\phi} = \frac{2\epsilon}{N} \frac{z}{\sqrt{1-z^2}} \cos \phi + \Lambda z, \quad (3b)$$

with the replacement  $\phi + 2k\bar{n} \rightarrow \phi$ . The total (conserved) energy is:

$$H = \frac{\Lambda z^2}{2} - \frac{2\epsilon}{N} \sqrt{1-z^2} \cos \phi \quad (4)$$

and the equations of motion (3) can be written in the Hamiltonian form  $\dot{z} = -\frac{\partial H}{\partial \phi}$  and  $\dot{\phi} = \frac{\partial H}{\partial z}$  with  $z$  and  $\phi$  canonically conjugate variables.

The Eqs.(3) have been studied in very different contexts, including polaron dynamics, where the dimer Eqs.(3) has been solved analytically [17], and in the Josephson dynamics of two weakly coupled Bose-Einstein condensates [18]. Eqs.(3) are those of a non-rigid pendulum:  $\phi$  is the angular position and  $z$  its conjugate momentum. The non-rigidity of the pendulum is due to its momentum dependent length.

The pendulum phase portrait,  $z-\phi$ , has been studied in [18]. Let us briefly recall the main results. We have a) oscillations around  $\langle \phi \rangle = 0$  and  $\langle z \rangle = 0$  (0-states); b) oscillations around  $\langle z \rangle \neq 0$  with running phase  $\langle \phi \rangle \propto t$  (self-trapped states); c) oscillations around  $\langle z \rangle = 0$  and  $\langle \phi \rangle = \pi$  ( $\pi$ -states); d) oscillations about  $\langle z \rangle \neq 0$  and  $\langle \phi \rangle = \pi$  (self-trapped  $\pi$ -states). Here  $\langle \dots \rangle$  stands for a time average. The stationary points of Eqs.(3),  $z = 0, \phi = 0$  (i.e.  $A = B$ ) and  $z = 0, \phi = \pi$  ( $A = -B$ ), correspond to time-independent solutions of Eq.(1),  $\psi_n = 2 \cos kn$  and  $\psi_n = 2i \sin kn$ , respectively.

To understand the meaning of these regimes in our system, we observe that the angular momentum is  $L(\tau) = i \sum_n (\psi_n \psi_{n+1}^* - c.c.) = 2Nz \sin k$ :  $\langle z \rangle = 0$  implies that the wave is completely reflected, and  $\langle z(\tau) \rangle \gg 0$  (or  $\langle z(\tau) \rangle \ll 0$ ) that the wave is only partially reflected by the impurity. The latter regime is given by a complete rotation of the pendulum about its center, and can be considered as a self-trapping of the angular momentum.

Equivalently, there is an effective energy barrier which forbids the complete reflection of the incident wave, and preserve its coherence. The observation of a persistent current is associated to a superfluid regime of the DNLS equation.

The situation changes in the (quasi-)continuum limit (which should not be confused with the  $N \rightarrow \infty$  limit). In this case phonons can be emitted only with quasi-momentum close to  $k$ , a condition which allows the applications of the Landau superfluidity criteria. The crossover between continuum and discrete limits is a very interesting one: We emphasize that the two-mode dynamics is crucially related to discreteness and nonlinearity, and disappears in the CNLS limit. Yet, there is a striking analogy: in both cases (in the Landau and in the "pendulum" criterion) the phonon emission out of the incident wave (which, therefore, dissipates its energy) can be inhibited by an effective energy barrier. The key difference lies on the corresponding spectrum of the emitted phonons, which leads to a completely different dynamics.

From the effective Hamiltonian (4) we find a critical value  $\Lambda_c$  for the pendulum oscillations about its center given by

$$H(\phi(0), z(0)) = 2\epsilon/N : \quad (5)$$

when  $\Lambda < \Lambda_c$ ,  $z$  oscillates around 0. When  $\Lambda = \Lambda_c$ , asymptotically  $z(\tau) \rightarrow 0$  and with  $\Lambda > \Lambda_c$ ,  $\langle z(\tau) \rangle \neq 0$ . In Fig.1 we plot the average value of the normalized angular momentum  $L(\tau)/L_0$  for different values of  $\Lambda/\Lambda_c$  and  $z(0) = 1$ ,  $\phi(0) = 0$ . The numerical solutions of Eq.(1) are in agreement with the two-mode approximation (3), dashed line. In the inset of Fig.1 we plot the normalized angular momentum vs. time for different  $\Lambda/\Lambda_c$ .

The fixed points of Eqs.(3) can be found by solving for  $\dot{z} = 0$ ,  $\dot{\phi} = 0$ . In particular, we have the non-trivial stationary (solitonic) solutions  $\phi = (2m + 1)\pi$ ,  $z = \pm\sqrt{1 - \frac{2\epsilon}{N\Lambda}}$  (with  $m$  integer). In Figs.2(a)-2(d) we compare the numerical and pendulum solutions for the normalized angular momentum and the phase, in the cases of  $\pi$  oscillations (a-b) and  $\pi$  stationary points (c-d).

The previous discussion can be extended to the case of many impurities: replacing the ansatz Eq.(2) in Eq.(1) we obtain:  $H = \frac{\Lambda z^2}{2} - \frac{2}{N}\sqrt{1 - z^2} \sum_n \epsilon_n \cos(\phi + 2kn)$ . After some algebra, the effective Hamiltonian becomes:

$$H = \frac{\Lambda z^2}{2} - \frac{2\bar{\epsilon}}{N}\sqrt{1 - z^2} \cos(\phi + \alpha) \quad (6)$$

with  $\bar{\epsilon}$  and  $\alpha$  given by the Fourier transform of the defects distribution:

$$\bar{\epsilon} e^{i\alpha} = \sum_n \epsilon_n e^{2ikn}. \quad (7)$$

The critical value  $\Lambda_c$  is given by Eq.(5) with the replacement  $\epsilon \rightarrow \bar{\epsilon}$ ;  $\phi_0 \rightarrow \phi_0 + \alpha$  [19]. It is also clear, from Eq.(7), that the system becomes transparent for

some particular distribution of defects. For instance, with an extended, step-like barrier ( $\epsilon_n = \text{constant}$  for  $\bar{n}_1 \leq n \leq \bar{n}_2$ ) of length 10 sites and with  $2k = \pi/5$ , we have  $\bar{\epsilon} = 0$ .

All the predicted regimes discussed so far have been found to be in agreement with our full numerical analysis. We considered different uniform random distributions of defects (e.g. all the  $\epsilon_n$  positive or negative or with zero mean value). The critical values of the nonlinearity found from the numerical solution of Eq.(1) and the comparison with the theoretical prediction for  $\Lambda_c$  from Eq.(5) is shown in Fig.3. In the inset of Fig.3 we plot  $L(\tau)/L_0$  as a function of time for various  $\Lambda$  and a random distribution of defects  $\epsilon_n$ . The excellent agreement between numerics and the solution of Eq.(6), and the robustness of the two-mode ansatz in the presence of an arbitrary distribution of defects, opens to the possibility of studying the competition between disorder (and Anderson localization) and nonlinearity from a new perspective. Eq.(6) is analytically solvable, yet still it contains all the essential ingredients to investigate the details of the superfluid - normal transition in the DNLS with impurities.

To conclude we briefly discuss the limits for recovering the CNLS equation (in an annular geometry) from the DNLS Eq.(1). Writing  $\Lambda = 2mg_0/\hbar^2 N$ ,  $\epsilon_n = V_n m L^2 / \hbar N^2$  and  $t = mL^2 / \hbar N^2 \tau$ , with  $V_n \equiv V(x = x_n)$  the defect potential in  $x_n$ ,  $L$  the length of the annulus and  $\tau$  the dimensionless time entering in Eq.(1), the CNLS is obtained in the limit  $N \rightarrow \infty$ . In particular, the critical value for the pendulum oscillations Eq.(5) becomes  $\Lambda_c = V_n m L^2 / \hbar N^3 \rightarrow 0$ . Therefore, approaching the continuous limit, the DNLS pendulum regime collapses to a (strongly) self-trapped state. This prevents the emission of phonons with opposite momenta with respect to the incident wave, whose energy will be eventually dissipated on a much longer time scale, according to the Landau argument.

Discussions with K. Ø. Rasmussen are acknowledged. This work has been supported by the U.S. DOE and the Cofinanziamento MURST.

---

- [1] A. C. Scott, *Nonlinear Science: Emergence and dynamics of coherent structures*, Oxford University Press (1999).
- [2] A. Sanchez, A. R. Bishop, SIAM Rev. **40**, 579 (1988).
- [3] T.V. Ramakrishnan, in *Chance and Matter*, Proceedings of the Les Houches Summer School, Session XLVI, edited by J. Souletie, J. Vannimenus, and R. Stora (North-Holland, Amsterdam, 1987), p. 213.
- [4] A.J. Leggett, Rev. Mod. Phys. **73**, 307 (2001)
- [5] H.S. Eisenberg *et al.*, Phys. Rev. Lett. **81**, 3383 (1998).
- [6] R. Morandotti *et al.*, Phys. Rev. Lett. **83**, 2726 (1999).
- [7] R. Morandotti *et al.*, Phys. Rev. Lett. **83**, 4756 (1999).
- [8] B.P. Anderson and M.A. Kasevich, Science **282**, 1686

(1998).

[9] S. Burger *et al.*, Phys. Rev. Lett. **86**, 4447 (2001).

[10] F. S. Cataliotti *et al.*, Science **293**, 843 (2001).

[11] O. Morsch, J.H. Müller, M. Cristiani, D. Ciampini and A. Arimondo, Phys. Rev. Lett. **87**, 140402 (2001)

[12] F. Dalfovo, S. Giorgini, L.P. Pitaevskii, and S. Stringari, Rev. Mod. Phys. **71**, 463 (1999).

[13] A. Trombettoni and A. Smerzi, Phys. Rev. Lett. **86**, 2353 (2001).

[14] Yu.S. Kivshar and M. Peyrard, Phys. Rev. **A46**, 3198 (1992).

[15] R. Scharf and A.R. Bishop, Phys. Rev. **A43**, 6535 (1991); Phys. Rev. **E47**, 1375 (1993).

[16] M.I. Molina, Phys. Rev. **B58**, 12547 (1998).

[17] V.M. Kenkre and D.K. Campbell, Phys. Rev. **B34**, 4959 (1986).

[18] A. Smerzi *et al.*, Phys. Rev. Lett. **79**, 4950 (1997); S. Raghavan *et al.*, Phys. Rev. **A59**, 620 (1999).

[19] As an example, we consider the case of a gaussian barrier  $\epsilon_n = (\epsilon/\sqrt{\pi}\sigma)e^{-(n-\bar{n})^2/\sigma^2}$  with width  $\sigma$ . The effective Hamiltonian is  $H = \frac{\Lambda z^2}{2} - (2\epsilon e^{-k^2\sigma^2}/N)\sqrt{1-z^2}\cos(\phi + 2k\bar{n})$  with the critical value obtained from (5) now given by  $\Lambda_c = 4\epsilon e^{-k^2\sigma^2}/N$ .

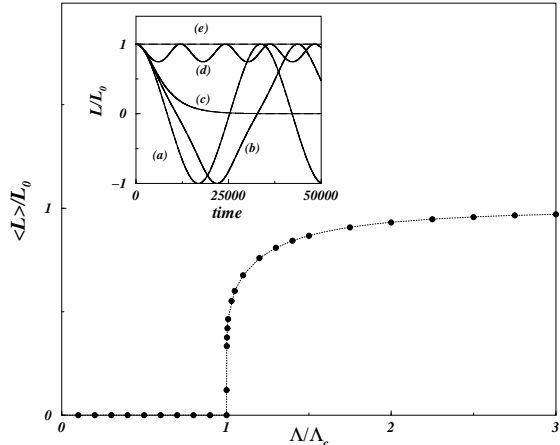


FIG. 1. Average value of the angular momentum  $L(\tau)$  (normalized to the initial value  $L_0$ ) vs. the nonlinear coefficient  $\Lambda/\Lambda_c$ , ( $\Lambda_c = 4\epsilon/N$ ), with  $\epsilon = 0.01$ ,  $N = 100$ ,  $z(0) = 1$ . The filled circles are the numerical solutions of Eq.(1), the dashed line is obtained from equations (3). Inset: normalized angular momentum vs. time for different values of  $\Lambda/\Lambda_c = 0.5, 0.75, 1, 1.5, 25$ , respectively, corresponding to (a), (b), (c), (d), (e).  $\phi(0) = 0$ .

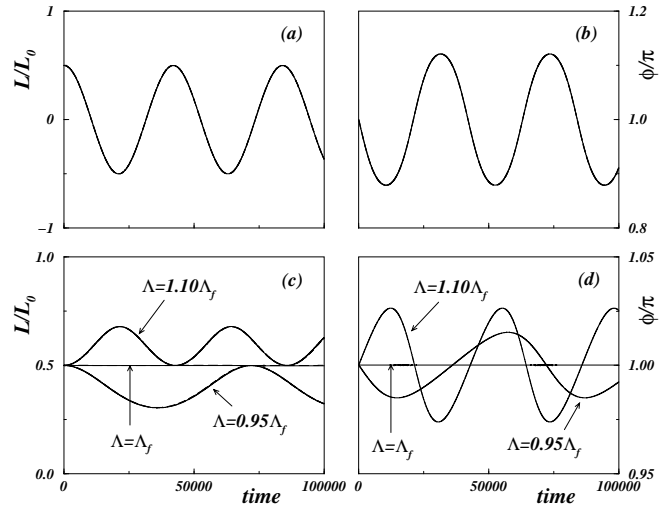


FIG. 2. Normalized angular momentum (a) and phase (b) vs. time for a  $\pi$ -state ( $\Lambda/\Lambda_c = 0.5$ ). In (c) and (d) we plot the same quantities for  $\Lambda_f = (2\epsilon/N)/\sqrt{1-z^2(0)}$  (the stationary solution of Eq.(3) with  $\phi = \pi$ ) and for  $\Lambda/\Lambda_f = 0.95, 1.10$ . In all cases solid (dashed) lines are for the numerical (variational) solution of Eq.(1) with  $\epsilon = 0.01$ ,  $N = 100$ ,  $z(0) = 0.5$ ,  $\phi(0) = \pi$ .

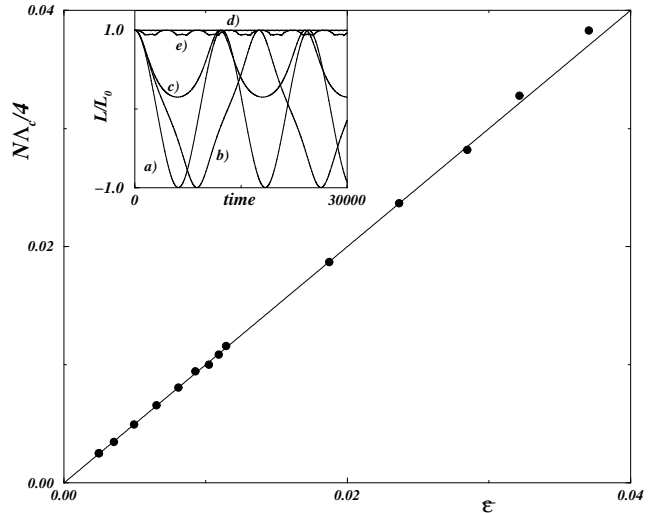


FIG. 3. Critical value  $\Lambda_c$  vs.  $\bar{\epsilon}$  for different random distributions of defects (and initial values  $z(0) = 1$ ,  $\phi(0) = 0$ ). Black circles: numerical solution of Eq.(1). Solid line: the analytical prediction  $\Lambda_c = 4\bar{\epsilon}/N$  with  $\bar{\epsilon}$  given by Eq.(7). Inset: angular momentum vs. time with a random distribution of defects for different values of  $\Lambda/\Lambda_c = 0.45, 0.90, 1.01, 10, 1000$  (corresponding to (a), (b), (c), (d), (e)). The sum of the strengths of the random impurities is 0.1.